NASA CR54075
T.I.S. R63SCW-31-3

N64-25803

Code-1 CAT. 09

35p.

TITLE: THIRD QUARTERLY REPORT OF STUDY OF CAPACITORS FOR STATIC INVERTERS AND CONVERTERS

(FEBRUARY 16, 1964 - MAY 16, 1964)

CONTRACT NO: NAS3-2788

PREPARED FOR THE

NATIONAL AERONAUTICS AND SPACE ADMINISTRATION

By J. F. Scoville

OTS PRICE

XEROX $ 3.60 ph

MICROFILM $ ______

GENERAL ELECTRIC

Copies of this report can be obtained from:

National Aeronautics and Space Administration
Office of Scientific and Technical Information
Washington, D. C., 20546
Attention: AFSS-A

NOTICE

NASA CR54075
T.I.S. R63SCW-31-3

TITLE: THIRD QUARTERLY REPORT OF STUDY OF CAPACITORS FOR STATIC INVERTERS AND CONVERTERS

CONTRACT NO: NAS3-2788

TECHNICAL MANAGEMENT
NASA-LEWIS RESEARCH CENTER
AUXILIARY POWER GENERATION OFFICE
FRANCIS GOURASH

PREPARED FOR THE

NATIONAL AERONAUTICS AND SPACE ADMINISTRATION

By J. F. Scoville

GENERAL ELECTRIC

TABLE OF CONTENTS

LIST OF FIGURES

#

SUMMARY

28803

This is the third quarterly report for the "Study of Capacitors for Static Inverters and Converters".

The objectives of this study are: (1) to establish capacitor AC characteristics and ratings for reliable operation in aerospace static inverter and converter applications; and (2) to facilitate the proper capacitor selection to minimize volume and weight consistent with maximum equipment performance and reliability.

This study was initiated because the significant capacitor volume, weight, power loss and reliability factors in space applications of static inverters and converters are at a premium and there are inadequate capacitor AC data and characteristics to enable consistent performance predictions.

General Electric's Specialty Control Department in Waynesboro, Virginia is conducting this study.

This report covers the work accomplished from February 16, 1964 through May 16, 1964 and contains:

a) Capacitor power factor and capacitance measurements at 25°C.

b) Commutating capacitor loss measurements while operating in an inverter.

c) Analysis of commutating capacitor losses.

author

INTRODUCTION

Capacitors being evaluated in this study are limited to those suitable for use in aerospace static inverters and converters operating in space environments. Inverter rating guides used in this capacitor study are 115/200 volt, 3-phase, 400 cycles, 0.1 to 10.0 kilowatt outputs with input voltage ranges from 25 to 105 volts D.C.

A need for the "Study of Capacitors for Static Inverters and Converters" was influenced by the stringent requirements imposed on capacitors by the operating nature of the equipment in the space environment and by the general lack of capacitor AC characteristics and data.

Appreciable heat is generated within commutating capacitors in static inverters because the commutating current pulse frequencies are approximately 5 kilocycles and usually some higher frequency ripple in the region of 50 kilocycles is superimposed. Transfer of the heat generated in these and filter capacitors is usually limited to conduction across their mounting surfaces to radiator cooling systems on spacecraft. Lack of adequate capacitor alternating current data and characteristics in aerospace inverter applications could result in appreciable weight and reliability factor penalties. Objectives of this study are to obtain AC characteristics and data of capacitors to facilitate proper selection for application in aerospace inverters and converters.

There are four (4) phases in this study: (1) Defining Capacitor State-of-the-Art Survey; (2) Conducting Capacitor State-of-the-Art Survey; (3) Experimental Testing of Capacitors; and (4) Capacitor Evaluation and Recommendations.

During the first and second quarterly report periods, the Capacitor State-of-the-Art Survey was defined and conducted. Sample quantities of metallized polycarbonate, polycarbonate/foil and metallized paper capacitors were procured for experimental testing. Results of the capacitor survey revealed that polycarbonate dielectric capacitors are considered state-of-the-art capacitors. These capacitors approach metallized paper capacitors in price, weight and volume and have lower dissipation factors than metallized paper.

This is the third quarterly report for the work accomplished between February 16, 1964 and May 16, 1964. During this period, the third phase of the study, Experimental Testing, was in progress. Test results included in this report are capacitance and power factor measurements versus frequency at 25°C, commutating capacitor loss measurements and analysis of commutating capacitor losses.

1.0 Capacitance and Dissipation Factor Tests

1.1 Purpose

Capacitance and dissipation factor values for polycarbonate and paper capacitors are being determined by test over a temperature range from - 55°C to + 85°C and frequency range from 400 cycles/second to 10 kilocycles. These data will provide equipment designers with characteristics that will facilitate proper selection of capacitors for aerospace inverter and converter applications. Temperature and frequency data are available for polycarbonate dielectric film, but polycarbonate capacitors are constructed from polycarbonate dielectric and other materials which can alter the capacitor characteristic.

1.2 Description of Tests

Capacitance values were determined with an impedance bridge constructed for these tests an elementary diagram is shown in Figure 1. Capacitance values measured with this bridge compared very favorably with values obtained with General Radio Model 716-C and Sprague Model 1W2 capacitance bridges.

Measurement of capacitor dissipation factors, that are within the tolerances of most commercially available bridges, were determined from calorimeter measurements. Comparison is then made with the impedance bridge measurements. The difference or correction factor between the two measurement methods was applied to the bridge measurement data. These bridge data are considered relative since unknown and stray capacitances are associated with most bridges and can introduce appreciable errors when measuring such low dissipation factors as 0.1 percent.

Use of the calorimeter is made in measuring the rate of heat being generated from an electrical circuit immersed in a fluid by observing temperature rise of the fluid versus time. Calibration of the calorimeter is accomplished by mounting resistors with known values of resistance in the calorimeter along with the capacitor to be tested. The resistor circuit is energized from a d.c. power supply and the current flow is accurately measured. Temperature rise of the calorimeter fluid is measured versus time. The calibration circuit is energized for a sufficiently long period to obtain a constant rate of temperature rise (i.e. after thermal inertia lag of the test specimen has been overcome.) A calorimeter calibration curve is shown in Appendix A, Figure A-1.

Elementary Diagram of Impedance Bridge

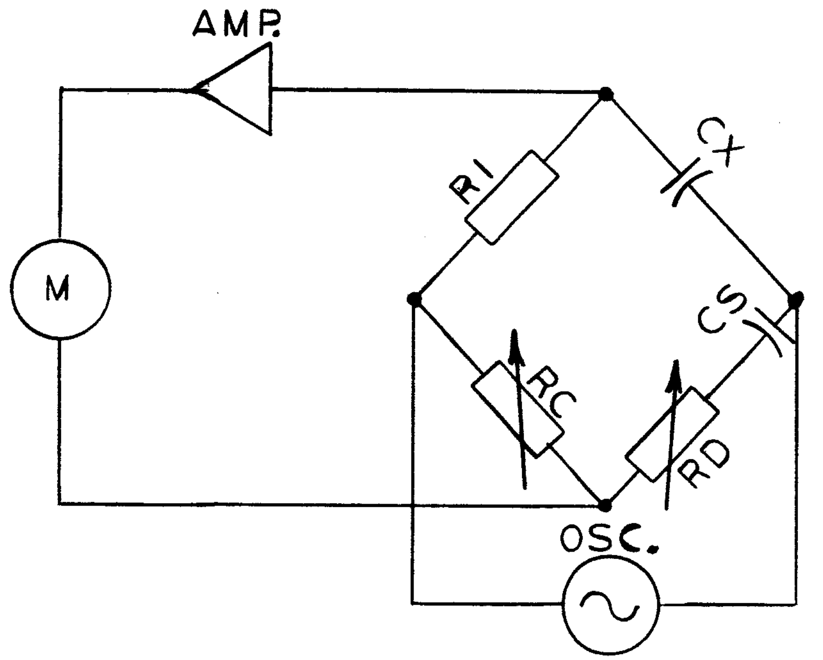

R1 = 99.7 OHMS; CS = .01 MFD., GEN. RADIO STD. 1409L

CX = Capacitor under test

RC = Adjustable resistance (switch, fixed resistors and a potentiometer)

RD = Adjustable resistance (switch, fixed resistor and a potentiometer)

AMP. - Battery operated, single stage, transistor amplifier

M - Harmonic Wave Analyzer - used as null detector

Dissipation Factor $= \frac{R_{cx}}{X_{cx}} = \frac{R_d}{X_{cs}} = RD\omega CS$

Where R_{cx} is the effective resistance of capacitor under test.

Capacitance: $\frac{R1}{RC} = \frac{X_{cx}}{X_{cs}}$ $\quad CX = \frac{CS(RC)}{R1}$

Figure 1

Calculation of the heat input to the calorimeter may be obtained from:

$$I^2R = \text{Watts} = {}^{\circ}C/\text{minute}$$

After calibrating the calorimeter, the capacitor is energized from a variable frequency power supply with simusoidal voltage. Capacitor dissipation factor (D.F.) losses are obtained from measurement of the RMS voltage across the capacitor, rate of temperature rise of the calorimeter fluid and use of the following calculations:

$$D.F. = \frac{\text{Watts}}{\text{VA}} \frac{(\text{rate of temperature rise/calibration rate of temperature rise})}{(\text{Capacitor voltage squared times } (2\pi f) \text{ times capacitance})}$$

Shown diagramatically

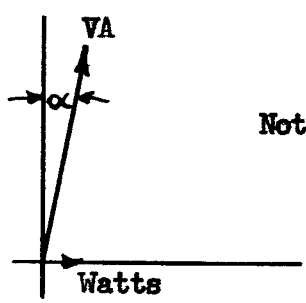

Note: Since the angle alpha is generally small, the dissipation factor is essentially the power factor.

Care was exercised to minimize the calorimeter heat loss rate by conducting tests only when the calorimeter fluid temperature was within $\pm$ 2°C of the calorimeter external ambient (24 - 26°C within the enclosure). Calorimeter fluid temperature was measured with a thermometer having 0.1°C graduations.

A picture of the test equipment used is shown in Figure 2. Figure 3 shows the mounting of a capacitor, calibrating resistors and thermometer to the top of a commercially available vacuum bottle, which is used as a calorimeter. The calorimeter shown in Figure 2 is in an enclosure to prevent room air currents from striking the external surfaces of the calorimeter that could alter the heat loss rate from the calorimeter.

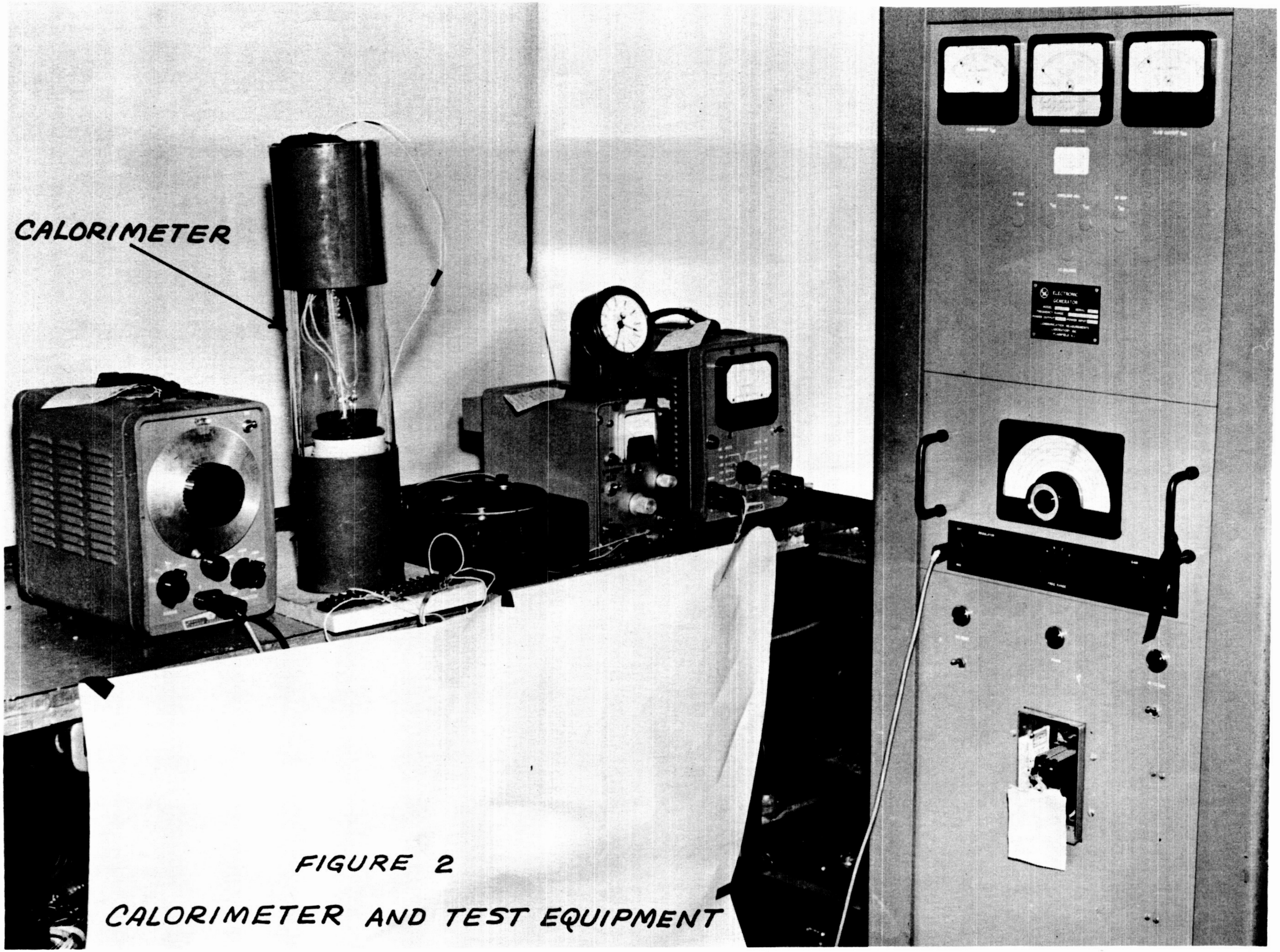

FIGURE 2

CALORIMETER AND TEST EQUIPMENT

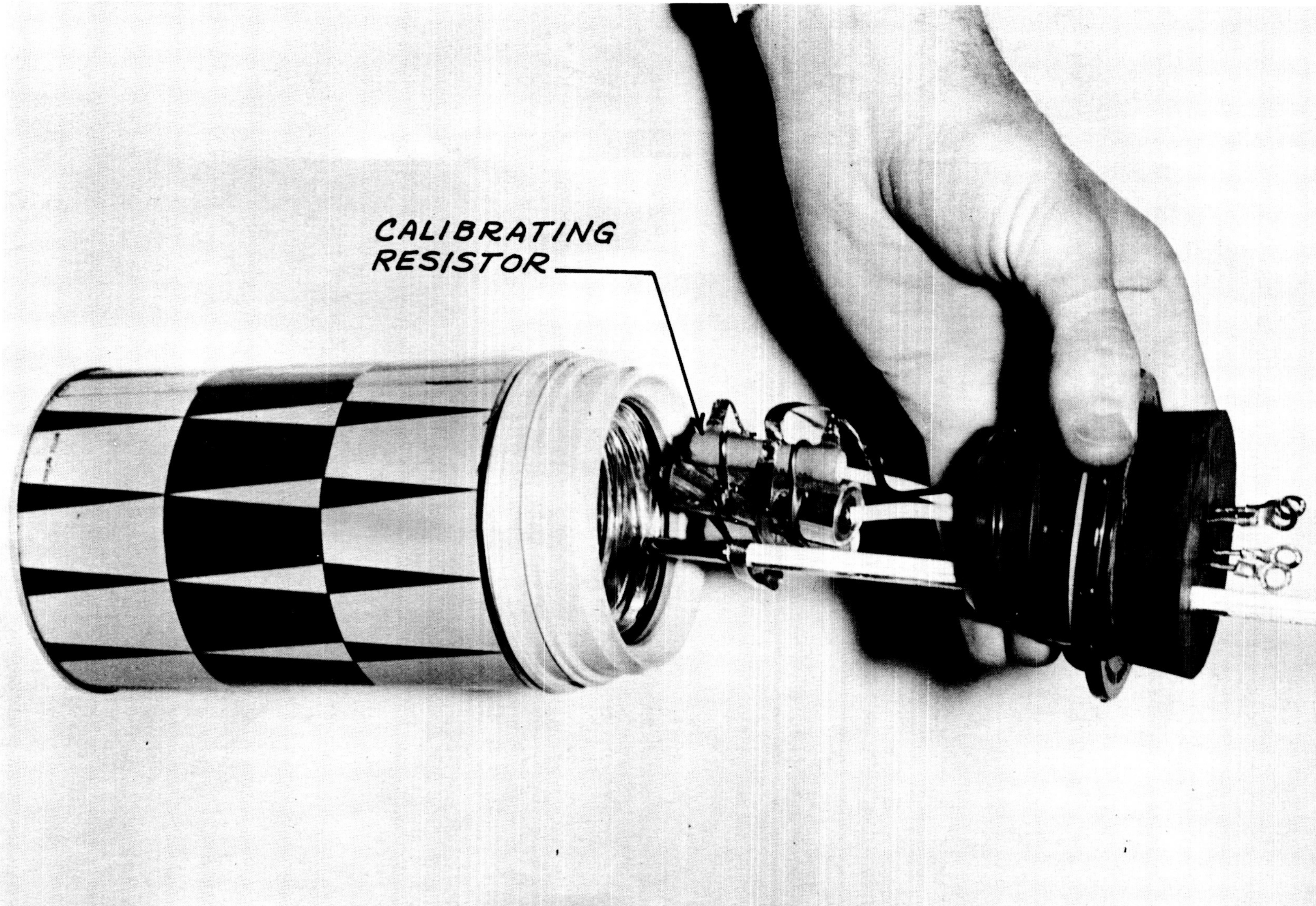

FIGURE 3

TEST SPECIMEN MOUNTING IN CALORIMETER

Bridge data for eighty-five (85) capacitors have been obtained for 25°C ambient, but the calorimeter tests to provide correction factors for the bridge data have not been completed. There are three (3) types of capacitors in this group of eighty-five: (1) metallized polycarbonate; (2) polycarbonate/foil; and (3) metallized paper.

1.3 Results of Tests

Capacitor dissipation factors for metallized polycarbonate in 25°C ambient are approximately 0.15 percent at 400 cycles/second and increase with frequency to approximately 1.0 percent at 10 kilocycles. Bridge and calorimeter data for three (3) capacitor ratings are tabulated in Tables A-1, A-2, and A3. Part of these data are plotted in Figures 4, 5, and 6 to illustrate the variation of the dissipation factors for a given capacitor rating. Similar data for metallized paper capacitors are tabulated in Table A-4 and plotted in Figure 6A for reference purposes.

Examination of the data in Tables A-1, A-2, and A-3 show an approximate capacitance increase of 2.0 percent from 400 cycles/second to 10 kilocycles.

Dissipation factor measurement for one of the capacitors listed in Table A-3 was extended to 50 kilocycles as shown in Figure 7 for reasons given in section 2.3 of this report. It is interesting to note the slope of the dissipation factor characteristic in Figure 7 at 50 kilocycles approximates the slope of 1 kilocycle.

2.0 Commutating Capacitor Tests

2.1 Purpose

Capacitor losses in commutating applications are of primary interest to an equipment designer selecting commutating capacitors for aerospace inverter and converter equipment designs. A method of correlating capacitor losses, while operating in commutating circuits, to capacitor losses measured with more conventional test equipment and sinusoidal voltages is desired. Such a correlation method would facilitate the proper capacitor type selection and preparation of capacitor specifications by the equipment designer to obtain predicted capacitor performance on a consistent basis.

2.2 Description of Test

A 2.5 microfarad, 400 VDC metallized polycarbonate capacitor was mounted in a calorimeter and it's dissipation factor determined

Dissipation Factor for 1.0 MFD Metallized Polycarbonate Capacitor

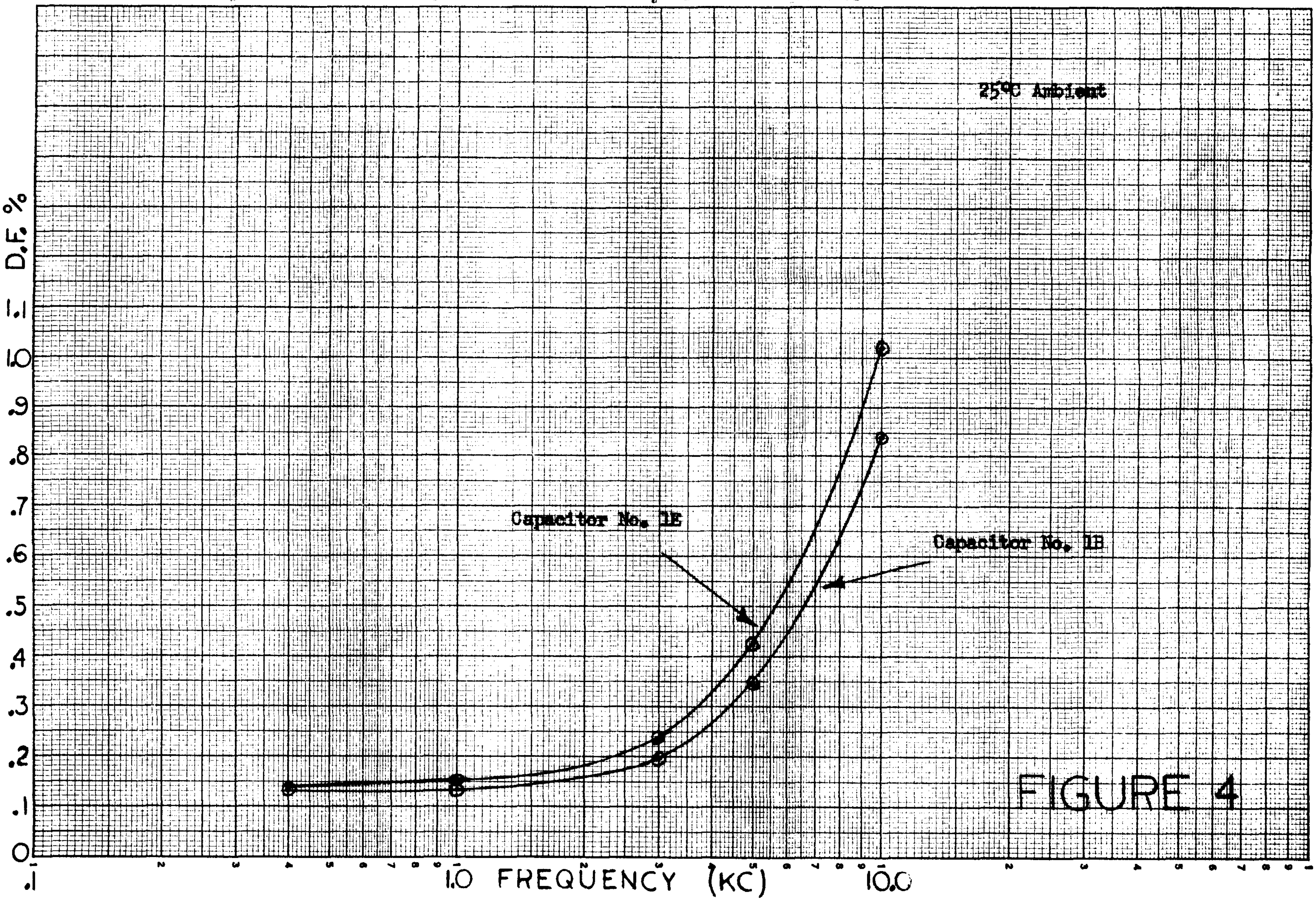

Dissipation Factor for 2.0 MFD Metallized Polycarbonate Capacitor

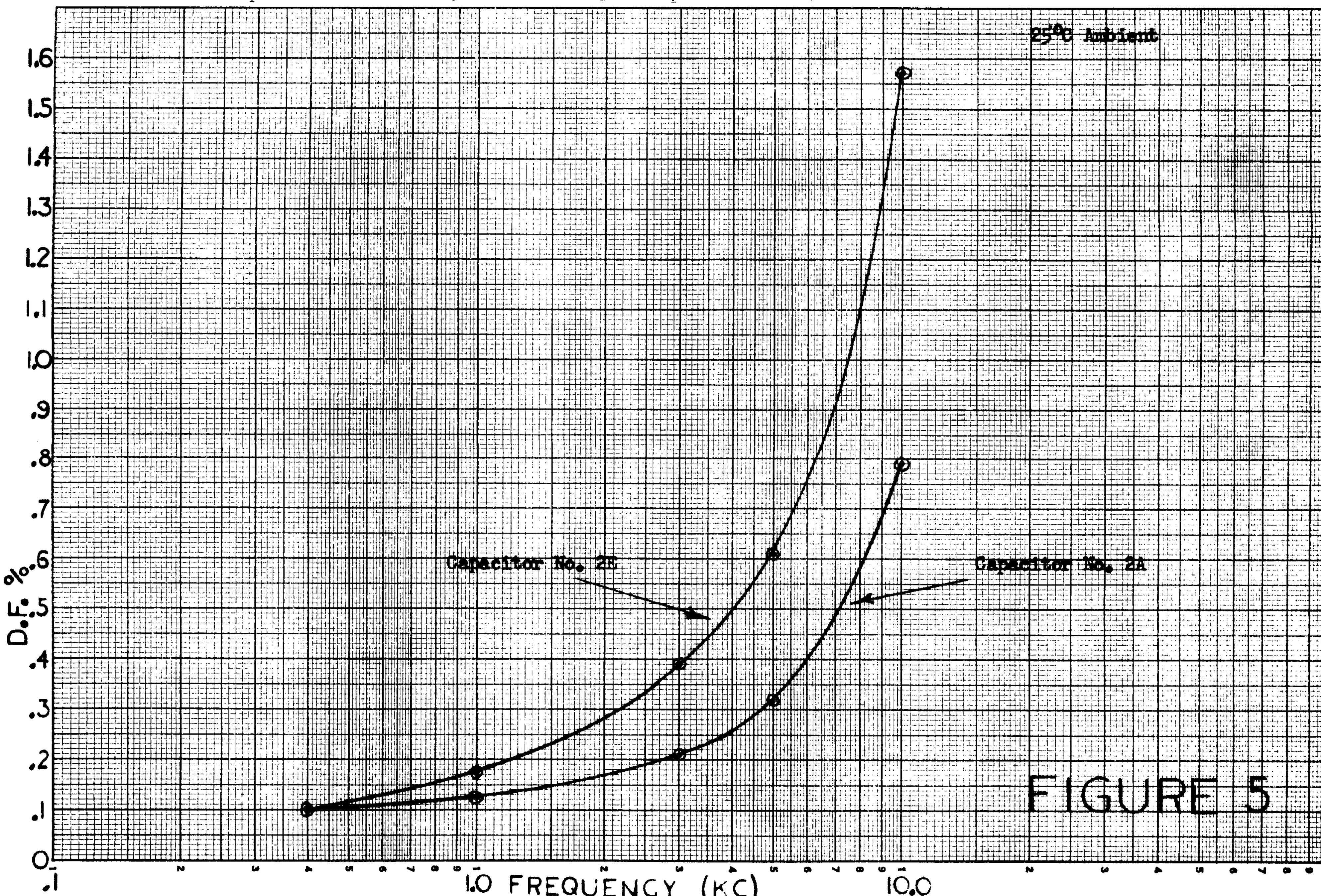

FIGURE 5

Dissipation Factor for 2.5 MFD Metallized Polycarbonate Capacitor

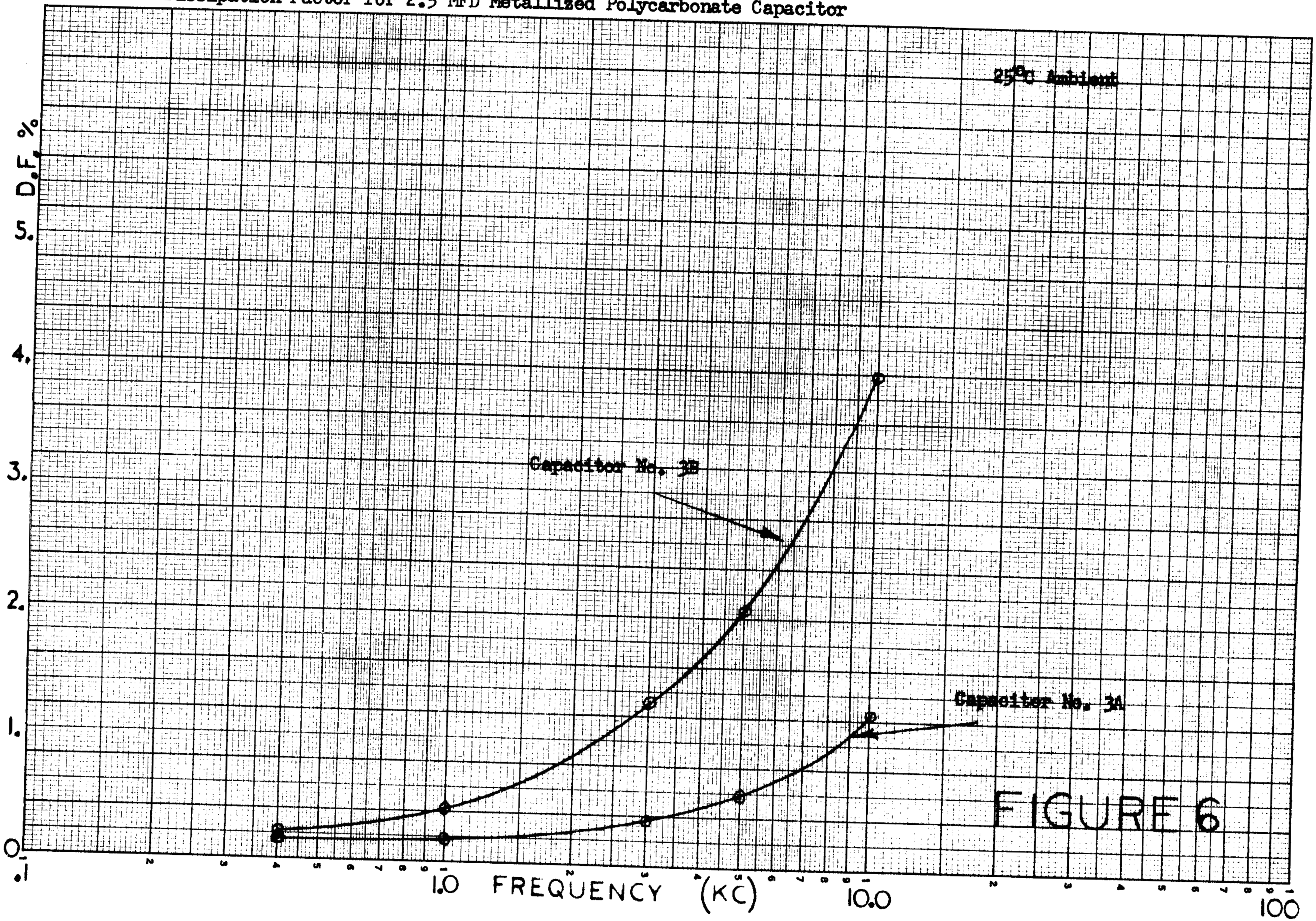

FIGURE 6

Dissipation Factor for 2.0 MFD Metallised Paper Capacitor

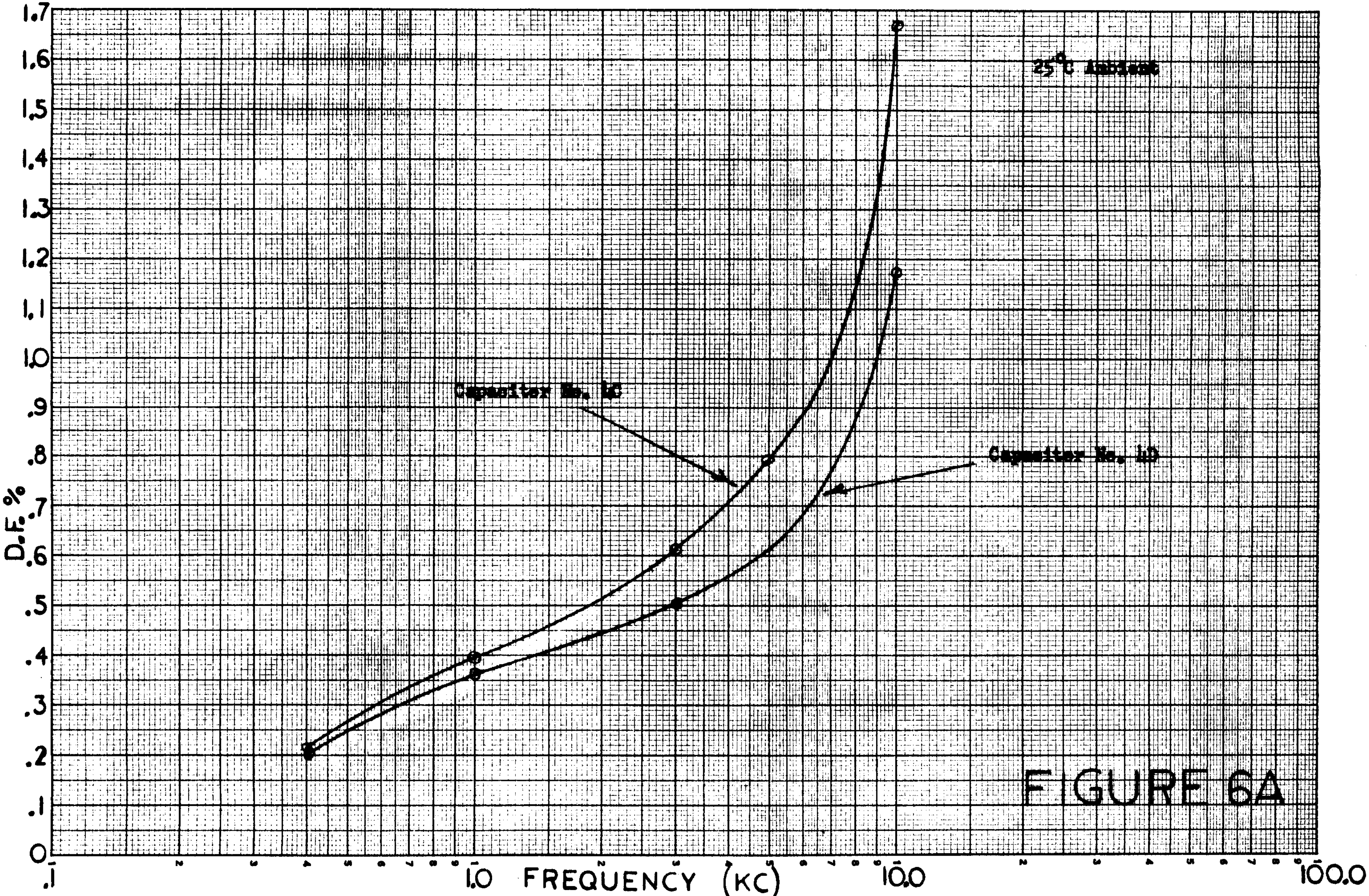

FIGURE 6A

utilizing sinusoidal voltages over a frequency range from 400 cycles/second to 50 kilocycles in a 25°C ambient.

While mounted in the calorimeter, the capacitor was connected to a static inverter and operated as a commutation capacitor. The capacitor heat loss was calculated from the calorimeter measurements. Calibrated oscilloscope pictures of the capacitor voltage and current waveforms were obtained during this test for use in analysis of the capacitor losses.

2.3 Results of Test

The dissipation factor of the commutating capacitor was approximately 9 percent at 50 kilocycles in a 25°C ambient. The dissipation factor versus frequency characteristic is shown in Figure 7.

Actual commutating capacitor losses while operating in the inverter circuit were 0.91 watts and the capacitor voltage and current waveforms, during this test, are shown in Figure 8. The encircled portions of the waveforms in Figure 8 were subjected to analysis, as described in section 3.0 to determine the RMS voltage and currents. A detailed wave analysis was considered necessary because the waveforms contain a significant amount of ripple.

3.0 Analysis of Commutating Capacitor Losses

3.1 Method of Analysis

Portions of the voltage and current waveforms that are encircled in Figure 8 were subjected to the following method of analysis to determine RMS volt-amperes of the commutating capacitor:

1) Voltage and current values from expanded portions of the waveforms as shown in Figures 9 and 10 were scaled at 5 microsecond ordinates as illustrated in Figure 9. These scaled values were squared and replotted as squared voltage and current curves.

2) A polar planimeter was then used to measure the areas under these new curves (i.e. volt^2-seconds or ampere^2-seconds).

3) The areas under the squared voltage and current waves were divided by the 400 cycle/second time base and the square root of the resultant was taken to obtain RMS values of the voltage and current.

COMMUTATING CAPACITOR WAVEFORMS

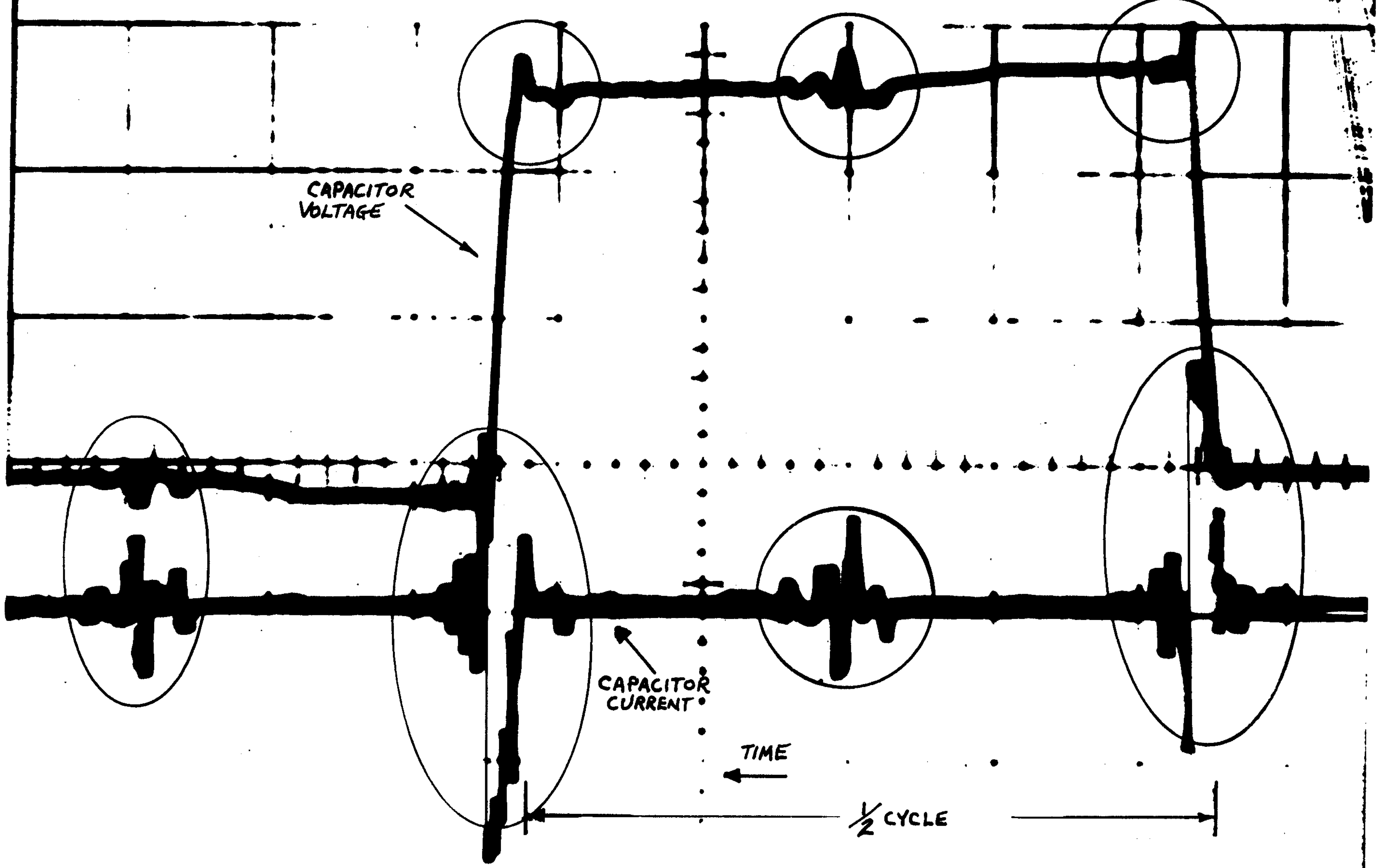

FIGURE 8

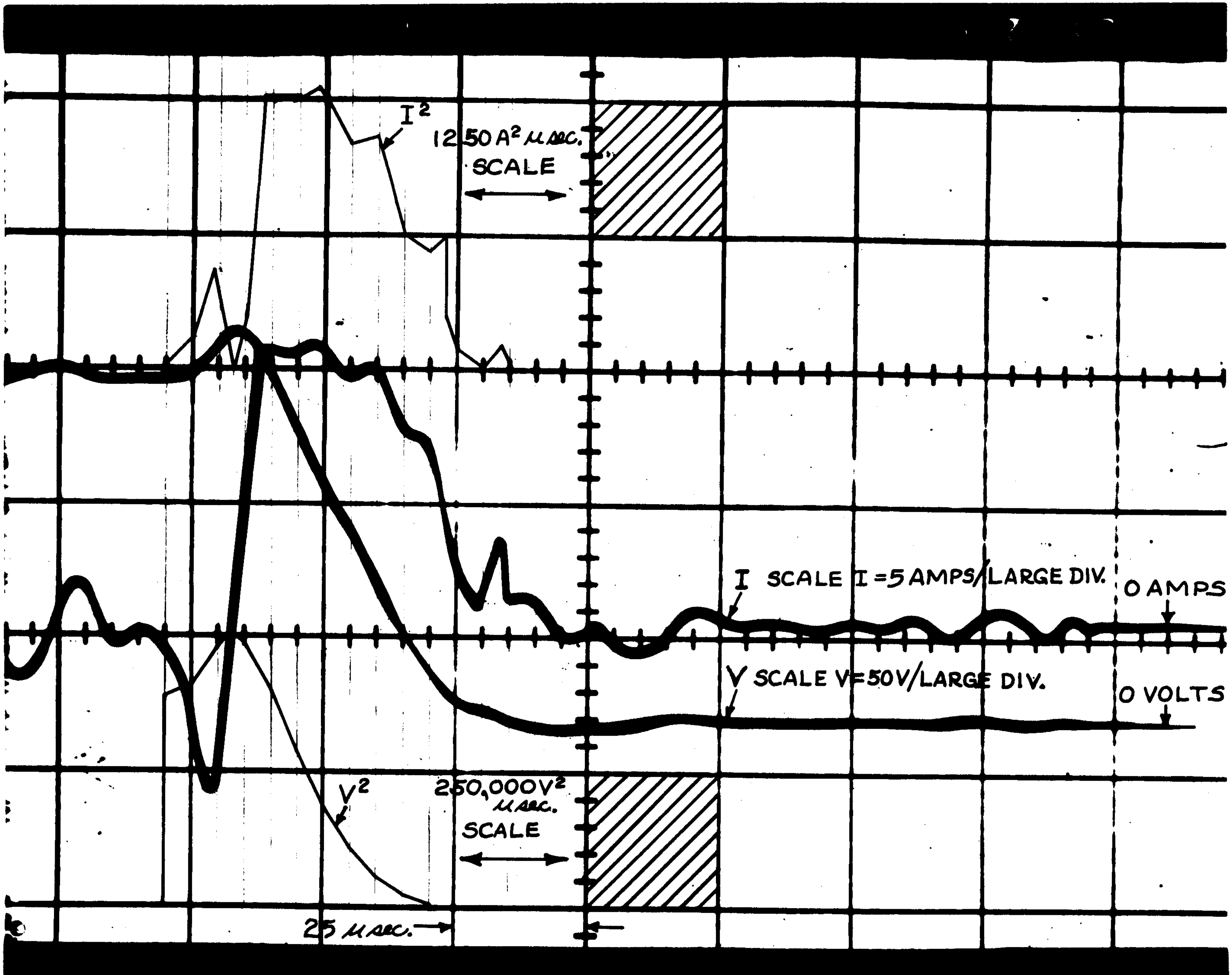

I^2
1250 A^2 μ sec.
SCALE
I SCALE I = 5 AMPS/LARGE DIV.
0 AMPS
V SCALE V = 50V/LARGE DIV.
0 VOLTS
V^2
250,000 V^2 μ sec.
SCALE
25 μ sec.

FIGURE 9

COMMUTATING CAPACITOR WAVEFORMS

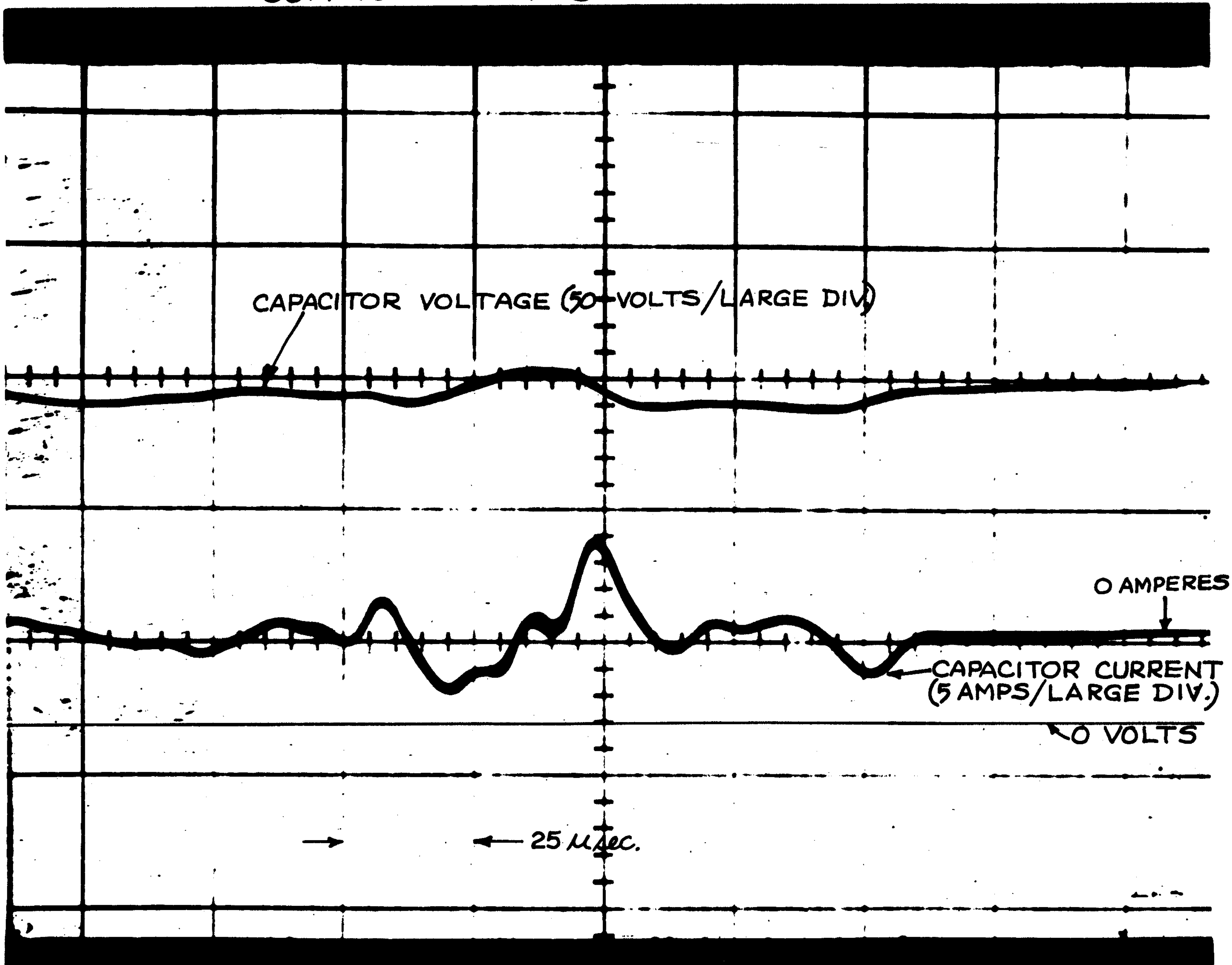

FIGURE 10

4) Since the basic frequency of the commutating current pulse is considerably different than the ripple, an assumption was made that a part of the capacitor losses are associated with this pulse volt-ampere value. It was assumed that the commutating current pulse conformed to a quarter sine wave function during an interval of 47.5 microseconds and had a peak value of 10.2 amperes. It was also assumed that the voltage function during this time interval conformed to a cosine function. From these assumptions, RMS voltage and current values were calculated for smooth waveforms as shown in Figure 11.

5) The RMS values obtained in 4) above were subtracted from those obtained in 3) above. The difference between these RMS voltage and current values was associated with the ripple frequency.

The RMS volt-ampere product, from the smooth commutating pulse, and the capacitor dissipation factor at the commutating pulse frequency yields that portion of the capacitor loss associated with the commutation pulse.

Taking the RMS volt-ampere product, associated with the ripple frequency, and the capacitor dissipation factor at the ripple frequency yields that portion of the capacitor loss attributed to the ripple.

3.2 Results of Analysis

The portion of the commutating capacitor loss associated with the commutation pulse was calculated to be 0.307 watts. The calculated loss attributed to the high frequency ripple was determined to be 0.662 watts. The sum of these two losses is 0.969 watts and compares very favorably with the 0.91 watts for the commutating capacitor loss as determined from calorimeter measurements.

Although the commutation pulse volt-amperes are 2.5 greater than the volt-amperes from the high frequency ripple the losses attributed to the commutation pulse are approximately one-half that from the high frequency ripple.

RMS CURRENT AND VOLTAGE FOR COMMUTATION PULSE

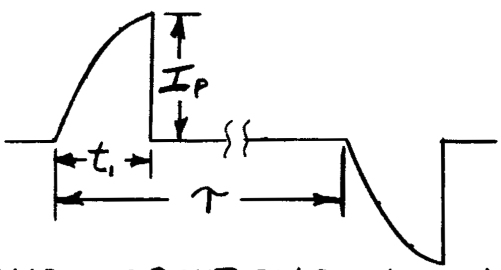

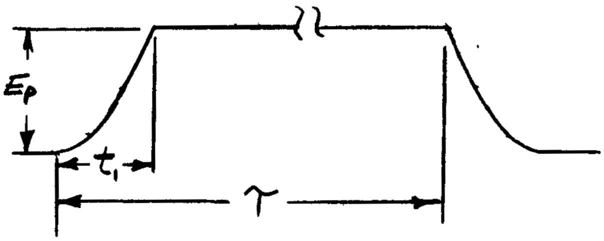

RMS CURRENT CALCULATION

RMS VOLTAGE CALCULATION

$t_1 = 47.5\ \mu\text{sec}$; $\tau = 1256\ \mu\text{sec}$; $f_0 = 400$ CPS ; $f_m = 5.28$ Kc

$\omega_0 = 2\pi f_0$; $\omega_m = 2\pi f_m$

$$I^2_{rms} = \frac{1}{\tau}\int_0^{t_1} i^2\,dt$$

$$i = I_p \sin \omega_m t$$

$$I^2_{rms} = \frac{I_p^2\omega_0}{\pi}\int_0^{\frac{\pi}{2\omega_m}} (\sin^2 \omega_m t)\,dt$$

$$= \frac{I_p^2\omega_0}{\pi}\left[\frac{t}{2} - \frac{t}{4\omega_m}\sin 2\omega_m t\right]_0^{\frac{\pi}{2\omega_m}}$$

$$= \frac{I_p^2\omega_0}{4\omega_m}$$

$$I_{rms} = 0.138\, I_p$$

$$I_p = 10.2$$

$$I_{rms} = 0.138(10.2) = 1.41$$

$$E^2_{rms} = \frac{1}{\tau}\int_0^{t_1} e^2\,dt$$

$$e = E_p(1 - \cos \omega_m t)$$

$$E^2_{rms} = \frac{E_p^2\omega_0}{\pi}\int_0^{\frac{\pi}{2\omega_m}} (1 - 2\cos \omega_m t + \cos^2 \omega_m t)\,dt$$

$$= \frac{E_p^2\omega_0}{\pi}\left[t - \frac{2}{\omega_m}\sin \omega_m t + \frac{t}{2} + \frac{1}{4\omega_m}\sin 2\omega_m t\right]_0^{\frac{\pi}{2\omega_m}}$$

$$= \frac{E_p^2\omega_0}{\omega_m}(0.75 - 0.636) = 0.114\,\frac{E_p^2\omega_0}{\omega_m}$$

$$E_{rms} = 0.093\, E_p$$

$$E_p = 127$$

$$E_{rms} = 0.093(127) = 11.8$$

FIGURE 11

Contract Distribution List

National Aeronautics & Space Administration
Lewis Research Center
21000 Brookpark Road
Cleveland, Ohio (44135)
Attn: B. Lubarsky MS 86-1 (1)
R. L. Cummings MS 86-1 (1)
N. T. Musial MS 77-1 (1)
J. J. Fackler MS 86-1 (1)
George Mandel MS 5-5 (3)
Billy G. Cauley MS 21-4 (1)
J. P. Quitter MS 4-9 (1)
C. S. Corcoran, Jr. MS 100-1 (1)
E. A. Koutnik MS 86-5 (1)
A. C. Herr MS 77-1 (1)
F. Gourash MS 86-1 (3)

National Aeronautics & Space Administration
Goddard Space Flight Center
Greenbelt, Maryland
Attn: F. C. Yagerhofer (1)
H. Carleton (1)

National Aeronautics & Space Administration
Marshall Space Flight Center
Huntsville, Alabama
Attn: James C. Taylor (M-ASTR-R) (1)
Richard Boehme (M-ASTR-EC) (1)

National Aeronatucis & Space Administration
Manned Spacecraft Center
Houston, Texas
Attn: A. B. Eickmeir (SEDD) (1)

National Aeronautics & Space Adminstration
4th and Maryland Avenue, S.W.
Washington 25, D. C.
Attn: James R. Miles, Sr. (SL) (1)
P. T. Maxwell (RPP) (1)
A. M. Greg Andrus (FC) (1)

Naval Research Laboratory
Washington 25, D. C.
Attn: B. J. Wilson (Code 5230) (1)

Bureau of Naval Weapons
Department of the Navy
Washington 25, D. C.
Attn: W. T. Beatson (Code RAEE-52) (1)
Milton Knight (Code RAEE-511) (1)

Jet Propulsion Laboratory
4800 Oak Brove Drive
Pasadena, California
Attn: G. E. Sweetnam (1)

Diamond Ordnance Fuze Laboratories
Connecticut Avenue & Van Ness Street, N.W.
Washington, D. C.
Attn: R. B. Goodrich (Branch 940) (1)

U. S. Army Research & Development Laboratory
Energy Conversion Branch
Fort Monmouth, New Jersey
Attn: H. J. Byrnes (SIGRA/SL-PSP) (1)

Engineers Research & Development Laboratory
Electrical Power Branch
Fort Belvoir, Virginia
Attn: Ralph E. Hopkins (1)

Aeronautical Systems Division
Wright-Patterson Air Force Base
Dayton, Ohio
Attn: Capt. W. E. Dudley - ASRMFP-3 (1)

University of Pennsylvania
Power Information Center
Moore School Building
200 South 33rd Street
Philadelphia 4, Pennsylvania (1)

Duke University
College of Engineering
Department of Electrical Engineering
Durham, North Carolina
Attn: T. G. Wilson (1)

National Aeronautics & Space Administration
Scientific and Technical Information Facility
Box 5700
Bethesda 14, Maryland
Attn: NASA Representative (6 copies ≁ 2 repro.)

AiResearch Division
Garrett Corporation
Cleveland Office
20545 Center Ridge Road
Cleveland 16, Ohio
Attn: W. K. Thorson

Westinghouse Electric Corporation
Aerospace Electrical Division
Lima, Ohio
Attn: Andress Kernick (1)

G. M. Defense Research Lab
General Motors Corporation
Santa Barbara, California
Attn: T. M. Corry (1)

The Martin Company
Baltimore, Maryland
Attn: Mike Monaco MS 3017 (1)

General Electric Company
Specialty Control Dept.
Waynesboro, Virginia
Attn: Mr. Lloyd Saunders (1)

Lear-Siegler, Incorporated
Power Equipment Division
P.O. Box 6719
Cleveland 1, Ohio
Attn: Mr. Robert Saslaw (2)

The Bendix Corporation
Bendix Systems Division
AnnArbor, Michigan
Attn: K. A. More (1)

The Bendix Corporation
Red Bank Division
1900 Hulman Building
Dayton, Ohio
Attn: R. N. Earnshaw (1)

VARO, Incorporated
2201 Walnut Street
Garland, Texas
Attn: J. H. Jordan (1)

Aerospace Corporation
P. O. Box 95085
Los Angeles 45, California
Attn: Library Technical Documents Group (1)

Engineered Magnetics Division
Gulton Industries, Incorporated
13041 Cerise Avenue
Hawthorne, California
Attn: Burton J. McComb (1)

AiResearch Mfg. Co.
Div. of the Garrett Co.
P.O. 5217
Phoenix, Arizona 85010
Attn: Mrs. J. F. Mackenzie, Librarian (1)

Separation of losses as described in the method of analysis provides a method of correlating commutating capacitor losses while operating in inverters and those obtained with sinusoidal waveform measurements. This analysis confirms the generally accepted rule that capacitor losses are a function of the frequencies with which a dielectric is worked.

Calculations of the RMS voltages and currents and capacitor losses from this analysis are contained in Appendix B.

4.0 Work Planned for Next Quarterly Report Period

It is planned to complete the capacitance and dissipation factor measurements for the eigthy-five (85) capacitors over an ambient temperature range from -55°C to +85°C and frequency range from 400 cycles/second to 10 kilocycles.

Approximately fifty (50) of these capacitors will be subjected to endurance or life testing at 85°C ambient with rated and above rated voltages for periods up to 1000 hours.

Vendors of capacitors, which exhibit significant variations of dissipation factors for a given capacitor rating, will be contacted and requested to determine the reasons for such significant variations.

Further testing for dissipation factors up to 80 kilocycles is planned as a result of the commutation capacitor loss analysis.

5.0 Conclusions

Dissipation factors for metallized polycarbonate capacitors are approximately one-half that for metallized paper capacitors in the range of frequencies from 400 cycles/second to 10 kilocycles.

A correlation between commutation capacitor losses while subjected to complex waveforms and from sinusoidal waveforms has been obtained. High frequency ripple on capacitor waveforms can cause excessive heating if the RMS volt-ampere products are appreciable.

Capacitors subjected to sinusoidal or commutation current duty applications should have maximum dissipation factors specified for the temperature and frequencies of interest to facilitate prediction of performance.

APPENDIX A

Capacitor Test Data

A calibration data curve for the calorimeter used in capacitor testing is shown in Figure A-1. These data used in plotting this curve were obtained by recording calorimeter fluid temperature versus time.

Figure A-2 illustrates a calorimeter data curve for a capacitor energized with a sinusoidal voltage of 25 volts RMS at 5 kilocycles in a 25°C ambient. Curves of this type were obtained at each test frequency for determining the capacitor dissipation factor characteristic.

Impedance bridge data for three (3) groups of five (5) capacitors each are tabulated in Tables A-1, A-2, and A-3. Dissipation factor correction factors were obtained by taking ratios of the bridge data at the test frequencies for the capacitor tested in the calorimeter and the other four (4) capacitors in the group times the calorimeter data.

Figure A-3 is a photograph of the impedance bridge and associated test equipment.

Calorimeter Calibration Data Curve

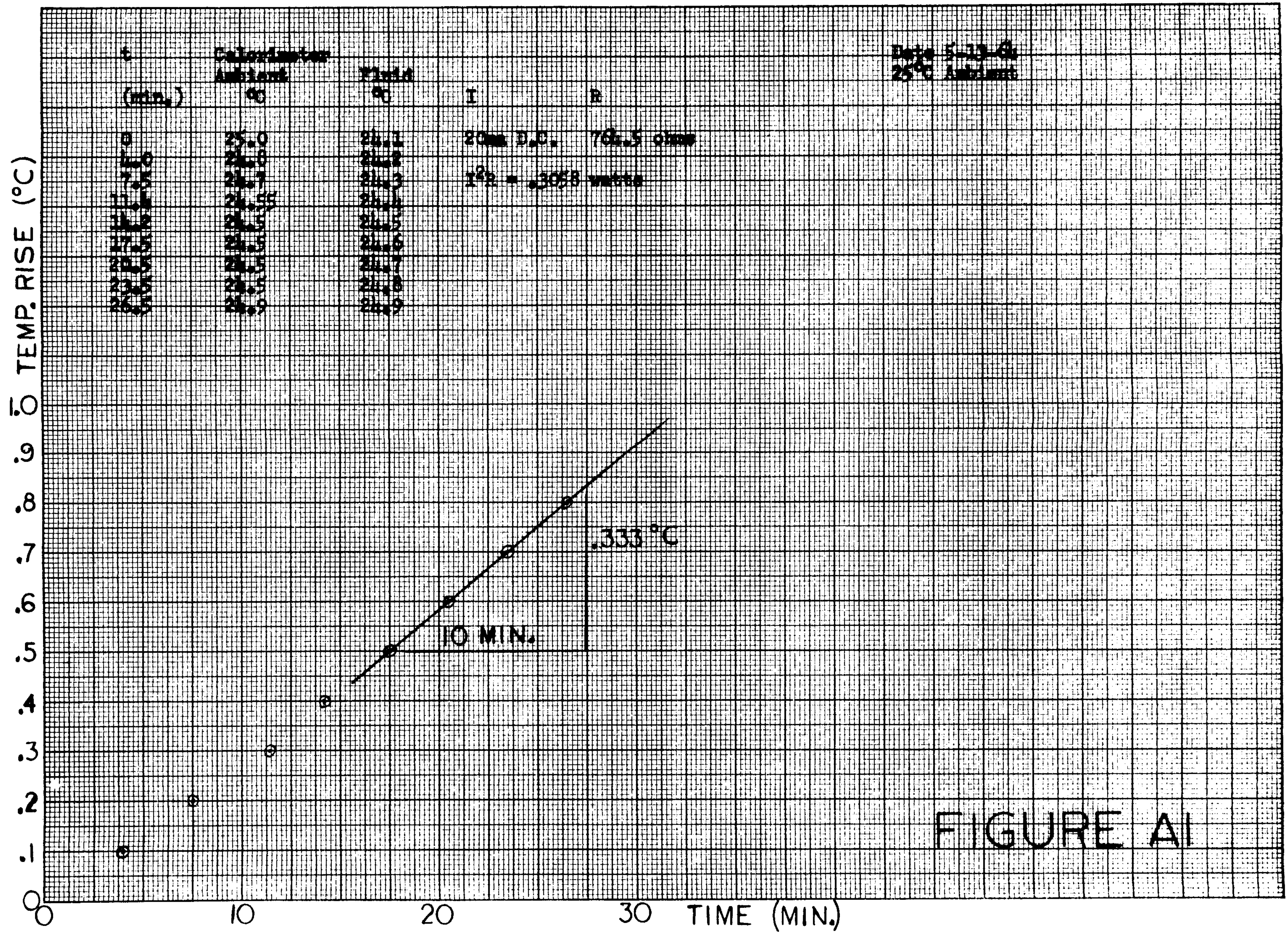

FIGURE A1

Calorimeter Data Curve for Capacitor at 5 Kilocycles

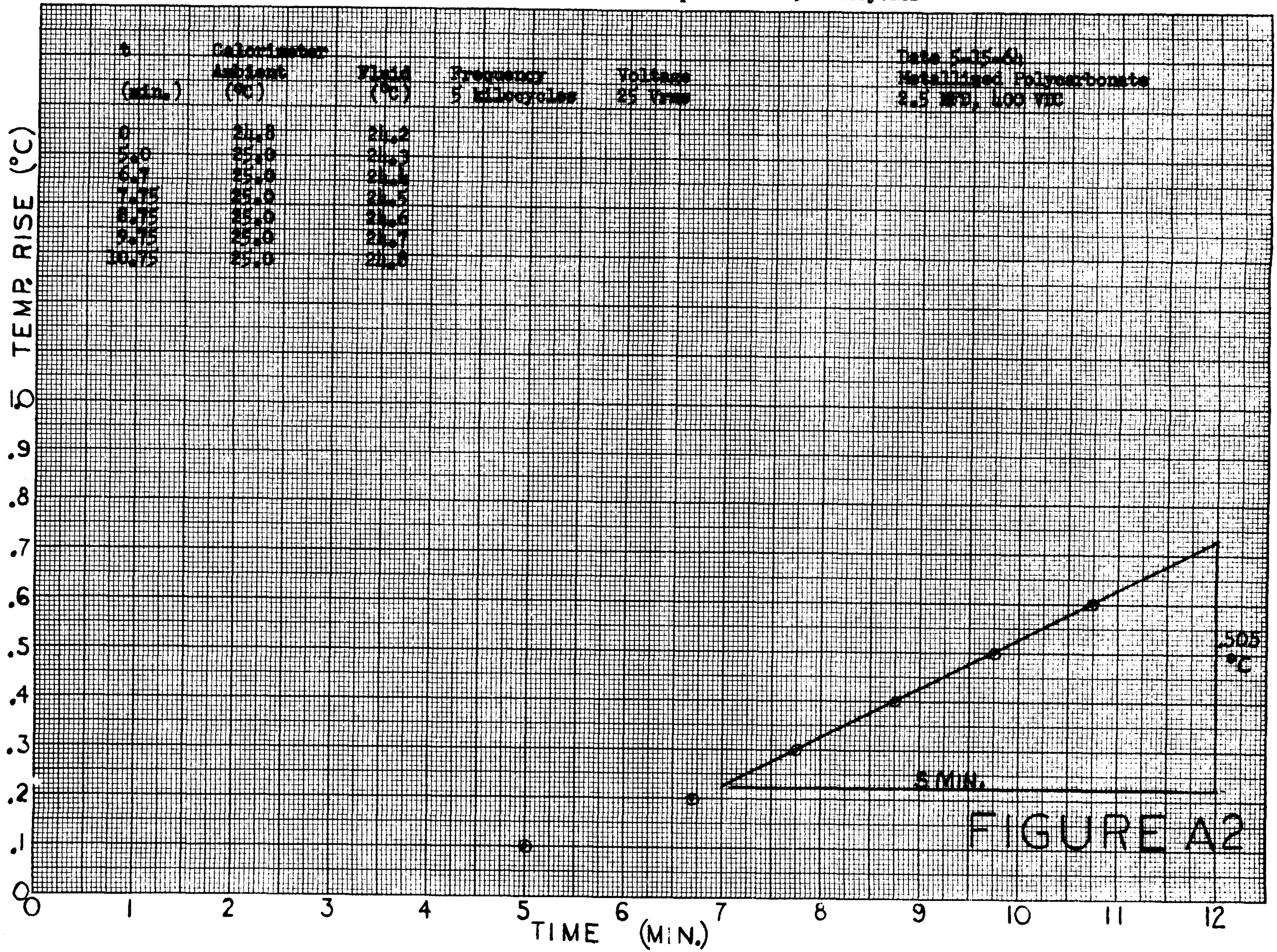

FIGURE A2

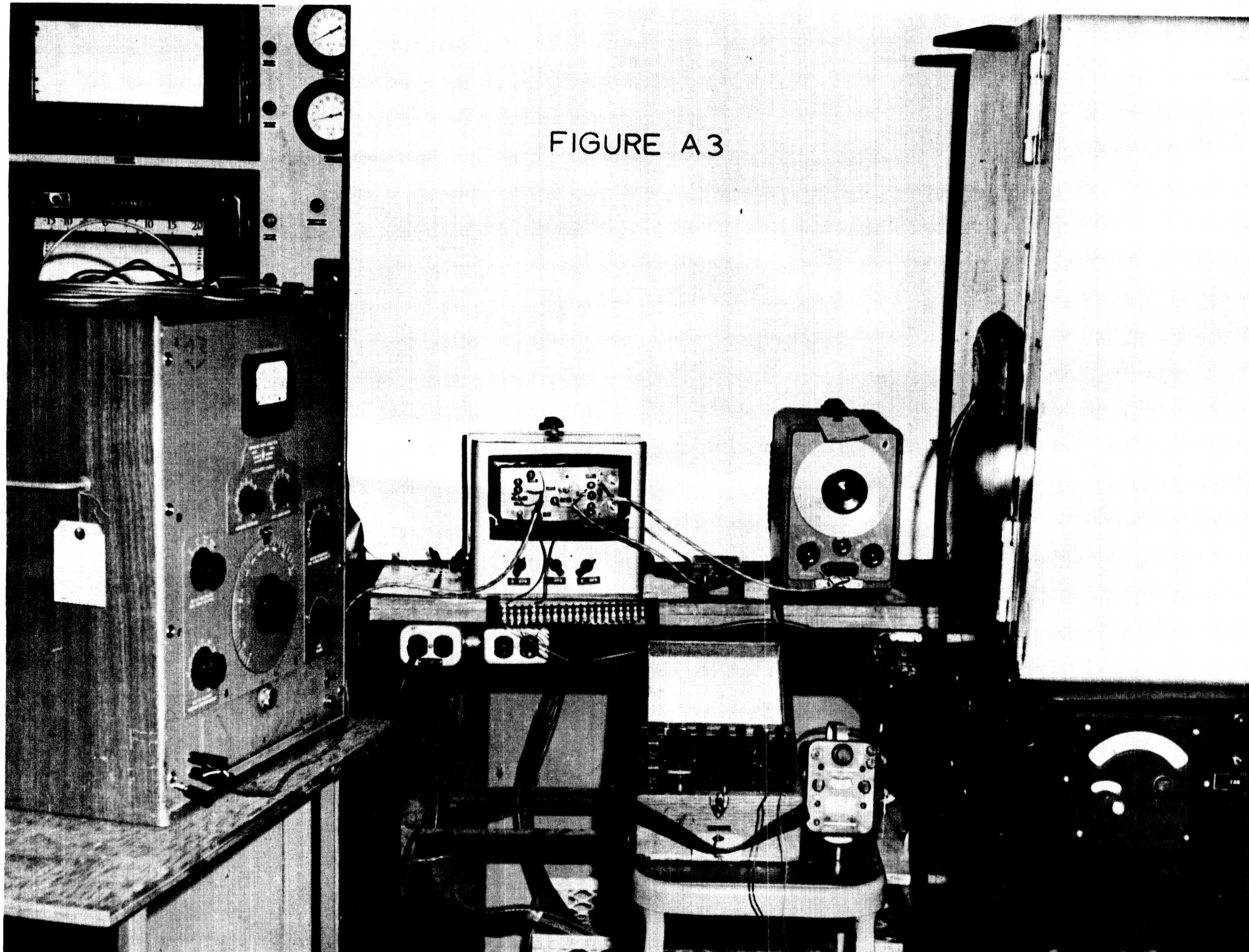

FIGURE A3

TABLE A-1

Capacitor Test Data for 1.0 MFD Metallized Polycarbonate Capacitors

Capacitor No.	Freq.	Bridge Measurement Rc (ohms)	Bridge Measurement Rd (ohms)	Calculated from Bridge Measurements C (MFD)	Calculated from Bridge Measurements D.F.% %	Calculated from Calorimeter Meas. D.F. (%)	Corrected Bridge D.F. (%)
1A	10 Kc	9890	17.70	.991	1.11	.975	—
	5 Kc	9820	18.49	.984	.581	.400	—
	3 Kc	9810	21.67	.983	.408	.222	—
	1 Kc	9771	57.5	.980	.361	.151	—
	400 cps	9626	291.0	.965	.731	.142	—
1B	10 Kc	9960	15.26	.998	.958	—	.840
	5 Kc	9860	16.13	.988	.507	—	.343
	3 Kc	9831	19.46	.986	.367	—	.198
	1 Kc	9814	50.24	.984	.316	—	.132
	400 cps	9675	267.1	.970	.671	—	.130
1C	10 Kc	10,030	15.46	1.01	.971	—	.852
	5 Kc	9,980	16.71	1.00	.525	—	.362
	3 Kc	9,962	19.42	.999	.366	—	.199
	1 Kc	9,930	52.51	.995	.330	—	.138
	400 cps	9.790	262.6	.981	.660	—	.903
1D	10 Kc	9,730	16.16	.975	1.02	—	.895
	5 Kc	9,670	17.19	.969	.540	—	.372
	3 Kc	9,648	20.14	.967	.379	—	.206
	1 Kc	9,629	56.14	.965	.353	—	.148
	400 cps	9,492	269.2	.952	.676	—	.131
1E	10 Kc	9,700	18.47	.952	1.16	—	1.020
	5 Kc	9,650	19.56	.967	.614	—	.424
	3 Kc	9,640	22.72	.966	.428	—	.233
	1 Kc	9,610	57.53	.963	.361	—	.151
	400 cps	9,476	274.7	.950	.690	—	.134

TABLE A-2

Capacitor Test Data for 2.0 MFD Metallized Polycarbonate Capacitors

Capacitor No.	Freq.	Bridge Measurement Rc (ohms)	Bridge Measurement Rd (ohms)	Calculated from Bridge Measurements C (MFD)	Calculated from Bridge Measurements D.F.% %	Calculated from Calorimeter Meas. D.F. (%)	Corrected Bridge D.F. (%)
2A	10 Kc	22,320	26.24	2.238	1.65	—	.790
	5 Kc	22,000	26.88	2.206	.844	—	.318
	3 Kc	21.920	28.51	2.198	.537	—	.209
	1 Kc	21,860	55.15	2.192	.346	—	.124
	400 cps	21,730	210.6	2.179	.529	—	.095
2B	10 Kc	22,320	39.87	2.238	2.50	—	1.200
	5 Kc	22,010	40.66	2.207	1.28	—	.482
	3 Kc	21,950	42.29	2.201	.797	—	.312
	1 Kc	21,890	68.52	2.195	.430	—	.154
	400 cps	21,770	220.8	2.183	.555	—	.100
2C	10 Kc	22,050	32.55	2.211	2.04	—	.975
	5 Kc	21,880	32.67	2.194	1.03	—	.388
	3 Kc	21,810	34.29	2.187	.646	—	.252
	1 Kc	21,750	61.61	2.181	.387	—	.138
	400 cps	21,640	213.4	2.170	.536	—	.096
2D	10 Kc	22,570	27.15	2.263	1.71	—	.818
	5 Kc	22,230	27.84	2.229	.874	—	.330
	3 Kc	22,160	29.61	2.222	.558	—	.218
	1 Kc	22,100	55.46	2.216	.348	—	.124
	400 cps	21,970	202.7	2.203	.509	—	.092
2E	10 Kc	21,910	52.26	2.197	3.28	1.57	—
	5 Kc	21,600	51.62	2.166	1.62	.61	—
	3 Kc	21,530	53.27	2.159	1.00	.39	—
	1 Kc	21,470	79.41	2.153	.499	.178	—
	400 cps	21,340	230.6	2.140	.579	.104	—

TABLE A-3

Capacitor Test Data for 2.5 MFD Metallized Polycarbonate Capacitors

Capacitor No.	Freq.	Bridge Measurement Rc (ohms)	Bridge Measurement Rd (ohms)	Calculated from Bridge Measurements C (MFD)	Calculated from Bridge Measurements D.F.% (%)	Calculated from Calorimeter Meas. D.F. (%)	Corrected Bridge D.F. (%)
3A	10 Kc	27,550	28.82	2.763	1.81	—	1.24
	5 Kc	27,040	28.80	2.712	.904	—	.577
	3 Kc	26,950	30.18	2.703	.569	—	.363
	1 Kc	26,860	54.18	2.688	.340	—	.178
	400 cps	26,750	200.2	2.683	.503	—	.166
3B	10 Kc	26,950	92.87	2.703	5.83	—	3.980
	5 Kc	26,820	103.4	2.690	3.25	—	2.060
	3 Kc	26,810	108.1	2.689	2.04	—	1.300
	1 Kc	26,780	133.3	2.686	.837	—	.436
	400 cps	26,650	271.5	2.668	.682	—	.225
3C	10 Kc	27,100	28.20	2.718	1.77	—	1.215
	5 Kc	26,600	28.44	2.668	.893	—	.569
	3 Kc	26,510	30.18	2.658	.369	—	.233
	1 Kc	26,440	55.35	2.651	.348	—	.183
	400 cps	26,320	200.2	2.639	.503	—	.166
3D	10 Kc	27,310	87.15	2.739	5.47	3.740	—
	5 Kc	26,920	87.60	2.700	2.75	1.750	—
	3 Kc	26,820	88.94	2.690	1.68	1.070	—
	1 Kc	26,800	112.8	2.688	.708	.370	—
	400 cps	26,640	253.7	2.672	.637	.210	—
3E	10 Kc	27,230	30.10	2.731	1.89	—	1.292
	5 Kc	26,730	30.72	2.681	.965	—	.613
	3 Kc	26,630	32.22	2.671	.607	—	.386
	1 Kc	26,550	56.43	2.662	.354	—	.186
	400 cps	26,420	194.3	2.649	.489	—	.162

TABLE A-4

Capacitor Test Data for 2.0 MFD Metallized Paper Capacitors

Capacitor No.	Freq.	Bridge Measurement Rc (ohms)	Bridge Measurement Rd (ohms)	Calculated from Bridge Measurements C (MFD)	Calculated from Bridge Measurements D.F.% %	Calculated from Calorimeter Meas. D.F. (%)	Corrected Bridge D.F. (%)
4A	10 Kc	18,500	40.12	1.855	2.52	—	1.205
	5 Kc	18,440	51.84	1.849	1.63	—	.613
	3 Kc	18,340	70.2	1.839	.325	—	.517
	1 Kc	18,380	163.9	1.843	1.03	—	.367
	400 cps	18,330	467.3	1.838	1.17	—	.210
4B	10 Kc	18,620	43.52	1.867	2.73	—	1.310
	5 Kc	18,440	55.49	1.849	1.74	—	.657
	3 Kc	18,430	72.25	1.848	1.36	—	.530
	1 Kc	18,450	164.0	1.850	1.03	—	.367
	400 cps	18,420	450.8	1.847	1.32	—	.238
4C	10 Kc	19,460	55.54	1.951	3.49	—	1.670
	5 Kc	19,300	67.10	1.935	2.11	—	.793
	3 Kc	19,290	83.24	1.934	1.57	—	.612
	1 Kc	19,340	175.2	1.939	1.10	—	.393
	400 cps	19,280	466.0	1.933	1.17	—	.211
4D	10 Kc	18,810	39.21	1.886	2.46	—	1.175
	5 Kc	18,630	51.57	1.868	1.62	—	.610
	3 Kc	18,620	68.25	1.867	1.29	—	.502
	1 Kc	18,660	160.1	1.871	1.01	—	.362
	400 cps	18,600	450.6	1.865	1.13	—	.203
4E	10 Kc	18,720	40.52	1.877	2.55	—	1.220
	5 Kc	18,550	52.50	1.860	1.65	—	.621
	3 Kc	18,540	69.38	1.859	1.31	—	.511
	1 Kc	18,590	161.2	1.864	1.01	—	.362
	400 cps	18,540	447.5	1.859	1.12	—	.202

APPENDIX B

Analysis of Commutating Capacitor Losses

From Figure 9, the commutation current pulse duration is 47.5 microseconds. The shape of this pulse approximates a quarter sine wave with a frequency of

$$f = \frac{1}{4t} = \frac{1}{4(47.5)\times10^{-6}\text{sec}} = 5.28 \text{ kilocycles}$$

The approximate shape of the voltage waveform during the commutation current pulse interval is cosinusoidal. The RMS volt-ampere product for these approximate wave functions during the commutation interval is derived in Figure 11 and numerically is 16.6 volt-amperes.

Analysis of the RMS voltage and current from the commutating capacitor waveforms is described in section 3.1 of this report. Squared values for a portion of the voltage and current waveform are illustrated in Figure 9. The sums of the squared volt-second and ampere-second values from the waveform pictures are:

$$(1) \quad \frac{4,505,217 \text{ Volt}^2\text{-usec}}{2500 \text{ usec}} = 1820 \text{ volt}^2$$

$$(2) \quad \frac{6646 \text{ amp}^2\text{-usec}}{2500 \text{ usec}} = 2.655 \text{ amp}^2$$

$$V_{rms} = \sqrt{1820} = 42.6 \text{ volts}$$

$$I_{rms} = \sqrt{2.655} = 1.63 \text{ amps}$$

The capacitor loss associated with the commutation pulse at 5.28 kilocycle frequency from Figures 11 and 7 is:

$$VI\ (D.F.) = (11.8)\ (1.41)\ (.0185) = 0.307 \text{ watts}$$

Subtracting the 11.8 volts rms and 1.41 amps RMS during the commutation interval leaves:

$$42.6 - 11.8 = 30.8 \text{ Volts rms}$$
$$1.63 - 1.41 = 0.22 \text{ amps rms}$$

The product of the RMS voltage and current associated with the ripple and the capacitor dissipation factor determined with sinusoidal voltages at the ripple frequency yields:

(1) Dissipation Factor from Figure 7 for 80 kilocycles = 9.9%

(2) VI (D.F.) = (30.8) (0.22) (.099) = .671 watts

The sum of the watts attributed to the ripple and commutating pulse is:

0.307 watts (commutation pulse)
0.671 watts (ripple)
0.978 watts

The measured commutation capacitor loss in the calorimeter was 0.91 watts and favorable agreement, within 7.5 percent of this loss, was achieved with the described analysis.